CHAPTER 4

Reduction of MnO_2(birnessite) by Malonic Acid, Acetoacetic Acid, Acetylacetone, and Structurally-Related compounds

4.1 Abstract

This study examines rates and pathways for redox reactions between a synthetic MnO_2(birnessite) and thirteen organic compounds, including eight β-diketones, two β-ketocarboxylic acids, and three β-dicarboxylic acids. With β-diketones, high reactivity generally corresponds to high enol content, which is contributed by the presence of labile α-H atom(s). With β-dicarboxylic acids, malonic acid and dimethylmalonic acid are much more reactive than dimethylmalonic acid, indicating that a α-H is required for higher reactivity. Malonic acid oxidation via the conversion of a α-H into a α-OH to yield tartronic acid has been proposed based upon product analysis. For acetylacetone, acetoacetic acid, and malonic acid, the effect of pH on reactivity correlates well with the pH dependence of adsorption.

4.2 Introduction

Studies are underway in our laboratory in an effort to understand and predict rates of electron transfer between aliphatic organic compounds and manganese(III,IV) (hydr)oxides. The previous paper in this series *(1)* included rates of dissolved Mn^{II} production (R_0) for the following four organic substrates:

		R_0 (μM/hr)
Oxalic acid	HOOCCOOH	462
Pyruvic acid	$H_3C(C=O)COOH$	68
2,3-Butanedione	$H_3C(C=O)(C=O)CH_3$	30
Oxalic acid Dimethyl Ester	$H_3COOCCOOCH_3$	2.7

These rates were recorded using suspensions containing 200 μM synthetic MnO_2, 5.0 mM organic substrate, and 10.0 mM butyrate buffer (pH 5.0). Reductive dissolution reactions of this kind are believed to begin with organic substrate-surface precursor complex formation, which is an adsorption process, and then proceed to electron transfer. Free carboxylate groups facilitate reaction by facilitating precursor complex formation. The presence of proximal carbonyl (C=O) groups in all four compounds yields electronic delocalization via resonance, which lowers the activation barrier towards oxidation.

What happens when a methylene group ($-CH_2-$) is inserted between the proximal carbonyl groups of these four organic substrates, as illustrated by the four organic substrates listed below?

Malonic acid	$HOOCCH_2COOH$
Acetoacetic acid	$H_3C(C=O)CH_2COOH$
Acetylacetone	$H_3C(C=O)CH_2(C=O)CH_3$

Malonic acid Dimethyl Ester $H_3COOCCH_2COOCH_3$

The resonance afforded by proximal carbonyl groups is no longer possible, but keto-enol tautomerization and the acidity of the methylene C-H (i.e. alpha C-H) bond become important considerations.

What role does the α-CH play in the oxidation of these organic substrates by MnO_2(birnessite)? Can we relate organic reactivities to their physical-chemical properties, specifically keto-enol and protonation equilibria? To establish organic structure-reactivity relationships, we have carefully selected eight β-diketones, two β-ketocarboxylic acids, and three β-dicarboxylic acids for study (Tables 4.1 and 4.2), including the four organic substrates mentioned in the previous paragraph. The effect of pH on rates of organic reaction with MnO_2(birnessite) has been examined, providing additional property-reactivity information. Along with the identification of malonic acid oxidation products, some details regarding the molecular-level mechanism of malonic acid (and related analogues) oxidation are clarified.

Malonic acid is of considerable biogeochemical importance. Release of malonic acid by plant roots, bacteria, and fungi yields measurable concentrations in soil interstitial waters *(2-4)*. Acetoacetic acid is a metabolic byproduct *(5)*. β-diketones are synthetic compounds with numerous practical applications. Traditional applications mostly reside in the industrial field: metal complexes of β-diketones have been used as fuel additives *(6)*, as supercritical fluids for waste cleanup *(7)*, in superconducting thin film manufacturing *(8)*, and in production of catalysts *(9)*. Recently, the applications have been expanded to the medicinal field: small β-diketones, such as acetylacetone, serve as

intermediates in preparation of anticancer reagents and HIV inhibitors *(10-13)*, of which the functionality comes from the antioxidant action in the β-diketone moiety *(14, 15)*.

Substrate Properties: Keto-Enol and Protonation Equilibria.

Equilibrium Constants. The keto and enol tautomers are structural isomers that are conceptually related by the shift of a hydrogen or one or more π bonds. Compared to most simple ketones, the enol tautomers of β-diketones are relatively stable due to the intramolecular H-bonding and conjugation within the 6-membered ring *(16, 17)*. The α-hydrogens of β-diketones are often acidic as result of the charge stabilization by resonance, when deprotonates, the enolate anion forms.

Let us first consider organic compounds with two carbonyl groups β- to one another with a linking carbon bonded to at least one hydrogen. For the moment, let us assume that the compounds are symmetrical. Two tautomers are possible:

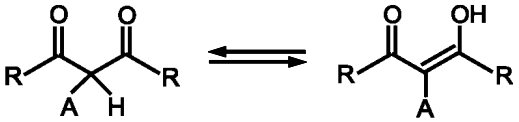

KH ⇌ EH

$$K_E = \frac{[EH]}{[KH]} \qquad (1)$$

In addition, a protonation/deprotonation reaction can be written for each of the two tautomers:

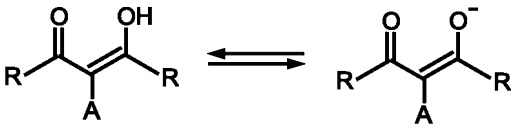

EH ⇌ E^- + H^+

$$K_a(EH) = \frac{[E^-][H^+]}{[EH]} \qquad (2)$$

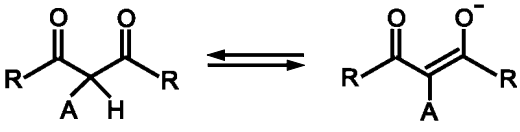

KH ⇌ E^- + H^+

$$K_a(KH) = \frac{[E^-][H^+]}{[KH]} \qquad (3)$$

Simple acid-base titrations fail to distinguish between EH and KH, and hence yield a composite protonation constant:

$$K_a^{app} = \frac{[H^+][E^-]}{[KH] + [EH]} = \frac{K_E K_a(EH)}{1 + K_E} = \frac{K_a(KH)}{1 + K_E} \quad (4)$$

Once K_a^{app} and K_E are known, $K_a(EH)$ and $K_a(KH)$ can be calculated using Equation 4. For asymmetric compounds ($R_1 \neq R_2$), a pair of enol structural isomers can be envisioned *(16, 18)*:

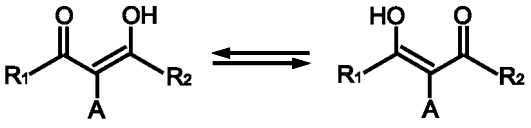

EH(1) EH(2)

$$K' = \frac{[EH(2)]}{[EH(1)]} \quad (5)$$

For each structural isomer there is a corresponding pK_a. Fortunately, in most instances one structural isomer is several orders of magnitude less abundant than the other and can be ignored, enabling us to use the reactions and equations developed for symmetric compounds.

$-R_1$ and $-R_2$ for some of the compounds listed in Table 4.2 can exist in more than one protonation level. It is necessary to adjust the depiction of the fully protonated species accordingly (e.g. KH_2^0 and EH_2^0 represent two fully protonated forms of acetoacetic acid, see Figure 4.1). Additional keto/enol tautomerization constants corresponding to each protonation level of the side group are required for a complete description of speciation.

Structural Criteria. As illustrated in Table 4.1, the keto-enol tautomerism and acidity of β-diketones in aqueous solution strongly depend on the substitution pattern, including γ- (represented by R_1 and R_2) and α- (represented by A and B) substituent

effects. Acetylacetone represents the fundamental structure of β-diketones in this study, and is used as the baseline for comparison of other structures. 3,3-dimethyl-2,4-pentanedione does not have an α-H, therefore enolization and deprotonation can not occur. For this reason, the comparisons with regard to pK_E ($-\log K_E$) and pK_a^{eq} values are made among all other β-diketones.

The K_E values depend upon steric, inductive and resonance effects caused by substituents *(16, 19)*. The lower the K_E value, the lower the enol content. Four structures below acetylacetone in Table 4.1 arise from substitution in the γ-position, that is, the $-CH_3$ group(s) of acetylacetone. The $-C_2H_5$ groups in 3,5-heptanedione only cause a slight decrease in the enol content, which is generally true for substitution by the weakly electron-donating alkyl groups in the γ-position *(16)*. The $-OCH_3$ group in methyl acetoacetate causes a considerable decrease in enol content because the strongly electron-donating $-OCH_3$ group disfavors the electron delocalization crucial for enol stabilization within the conjugated ring structure *(16, 19)*. An additional $-OCH_3$ group substitution causes a further decrease in enol content; with the result that the enol content in dimethyl malonate is too low to be measured in aqueous solution. The $-CF_3$ group in 1,1,1-trifluoro-2,4-pentanedione causes a significant decrease in enol content, which is surprising at the first glance. The $-CF_3$ group is strongly electron withdrawing because of both inductive and resonance effects. Generally, electron-withdrawing groups tend to stabilize the enol over the keto tautomer, because the resonance effect allows delocalization of π-electrons within the conjugated ring structure *(16, 19)*. The intrinsic enol stabilization effect of the $-CF_3$ group is, however, overwhelmed by its interaction with water. Intermolecular H-bonding between F atoms in 1,1,1-trifluoro-2,4-

pentanedione and H atoms in H_2O molecules causes the intramolecular H-bonding within the enol tautomer to break, which dramatically decreases the enol content *(19, 20)*. 3-Chloro-2,4-pentanedione and 3-ethyl-2,4-pentanedione arise from substitution at the α-position, that is, the H atom(s) of acetylacetone. The electron-withdrawing chloro substituent in 3-chloro-2,4-pentanedione considerably increases the enol content *(16, 19)*. Unlike the γ-C_2H_5 groups in 3,5-heptanedione, the α-C_2H_5 group in 3-ethyl-2,4-pentanedione dramatically decreases the enol content because the enol structure is sensitive to the steric hindrance brought about by α-alkyl groups *(16, 19, 21)*.

pK_a^{app} values depend upon the stability of the conjugate base (i.e. enolate anion E^-) of β-diketones. The more stable the conjugate base, the more readily the conjugate acid will lose a proton to form it, and thus the lower the pK_a^{app}. The rule of thumb is that electron-withdrawing groups stabilize the conjugate base; electron-donating groups destabilize the conjugate base *(22)*. The trend of pK_a^{app} values of structures other than 3,3-dimethyl-2,4-pentanedione follows this rule. The higher pK_a^{app} value of 3-ethyl-2,4-pentanedione than that of 3,5-heptanedione is caused by steric hindrance at the α-position, disfavoring deprotonation. The low pK_a^{app} value of 1,1,1-trifluoro-2,4-pentanedione suggests that H-bonding favors deprotonation, regardless of intermolecular or intramolecular H-bonding *(20)*.

As shown in Figure 4.2, compared to acetylacetone, the introduction of a carboxylic acid group in acetoacetic acid leads to a more complicated speciation, which has been discussed earlier. The strong electron-donating effect of the carboxylic -OH group *(23)* leads to much lower enol contents and the much higher pKa_2^{app} for the α-CH ($pKa_2^{app} > 14$). Hence, the two carboxylic -OH groups in β-dicarboxylic acids should

lead to much lower enol content than the corresponding β-ketocarboxylic acids. Enolization of malonic acid and methylmalonic acid has been addressed by several authors *(24, 25).* The enol content is too low to be measured in aqueous solution by current techniques.

4.3 Materials and Method

All solutions were prepared from reagent grade chemicals without further purification, and distilled, deionized water (DDW) with a resistivity of 18 MΩ-cm (Millipore Corp., Milford, MA). Filter holders (Whatman Scientific, Maidstone, England) were soaked in 1N ascorbic acid (Aldrich, Milwaukee, WI) and rinsed with distilled water and DDW. All bottles and glassware for MnO_2(s, birnessite) and MnOOH(s, manganite) suspensions were first soaked in 1N ascorbic acid and rinsed with distilled water. They were next put in a 4N nitric acid (J. T. Baker, Phillipsburg, NJ) bath overnight and rinsed with distilled water and DDW water prior to use.

4.3.1 Materials. Methylmalonic acid, dimethylmalonic acid, succinic acid, acetylacetone, 3,5-heptanedione, methyl acetoacetate, dimethyl malonate, 1,1,1-trifluoro-2,4-pentanedione, 3-chloro-2,4-pentanedione, 3,3-dimethyl-2,4-pentanedione, and 3-ethyl-2,4-pentanedione were purchased from Aldrich. Malonic acid, potassium mono-methyl malonate, and lithium acetoacetate were purchased from Fluka (Buchs, Switzerland). Tartronic acid was purchased from Alfa Aesar (Ward Hill, MA). Methyltartronic acid was purchased from Pfaltz & Bauer (Waterbury, CT). Potassium 4-sulfobenzoate (Aldrich), sodium butyrate (Aldrich), 2-morpholinoethansulfonic acid monohydrate (MES; Fluka), and 3-[N-morpholino]propanesulfonic acid (MOPS; Sigma,

St Louis, MO) were used as pH buffers for the reaction systems. HCl (hydrochloric acid), NaOH (sodium hydroxide) and NaCl (sodium chloride) were purchased from J. T. Baker. TiO_2(rutile) was obtained from TiOxide Corp (Cleveland, England), and the corresponding properties was summarized in Table S4.1.

Details regarding the synthesis and characterization of the preparation we will refer to as MnO_2 are provided elsewhere *(26)*. It was synthesized according to the method of Luo et al. *(27)* and consisted primarily of birnessite. A B.E.T. surface area of 174 m^2/g was determined using a freeze-dried sample. The average Mn oxidation state was found to be +3.78 based upon iodometric titration. If the Mn^{II} content is negligible, then the preparation consists of 22 % Mn^{III} and 78 % Mn^{IV}. The freeze-dried particles weighed 97.10 grams per mole of manganese.

Synthesis and characterization of the preparation referred to as MnOOH was described elsewhere *(1)*. In brief, MnOOH was synthesized according to the method of Giovanoli and Leuenberger *(28)* and stored in a flash-frozen state. X-ray diffraction and TEM images confirmed that the preparation was predominantly manganite, corresponding to a pure Mn^{III} phase. Freeze-dried MnOOH yielded a B.E.T surface area of 27.3 m^2/g. The freeze-dried particles weighed 91.5 grams per mole of manganese.

4.3.2 Experimental Setup. *Degradation Experiments.* All batch experiments were conducted in 100 mL polypropylene bottles in a constant temperature circulating bath at 25 ± 0.2 ^oC and stirred with Teflon-coated stir bars. 10 mM 4-sulfobenzoate (pH 3.0 and 3.5), 10 mM butyrate (pH 4.0, 4.5 and 5.0), MES (pH 6.0), or MOPS (pH 7.0) were employed to maintain constant pH. pH stability was verified by periodic measurement (Fisher Accumet 825MP meter with Orion Combination semi-micro probe;

NIST-traceable standards). pH buffer concentrations were high enough to serve an additional purpose, maintenance of constant ionic strength conditions. No additional electrolyte was added.

Solutions containing organic substrate and pH buffer (plus additional constituents, as appropriate) were sparged with Ar (BOC gases, Baltimore, MD) for one hour prior to MnO_2 or MnOOH addition. Sparging was turned off immediately before MnO_2 or MnOOH addition. Reactors were sealed, but not sparged during reaction. 4mL reaction suspension aliquots were collected at periodic intervals. Reactions were quenched by immediately filtering through 0.1 μm pore diameter track-etched polycarbonate filter membranes (Whatman). Total dissolved manganese in the filtered solutions was analyzed using flame atomic absorption spectrophotometry (AAS: Aanalyst 100, Perkin Elmer, Norwalk, CT). Mn AAS standard was purchased from Aldrich. Additional species in the filtered solutions were analyzed using capillary electrophoresis (see later section). Inorganic carbonate was not monitored due to possible losses arising from sparging.

Adsorption Experiments. Adsorption experiments were performed on a non-redox active TiO_2(rutile) surface. All experiments began by adding TiO_2 stock suspension, solution of the test compound (malonic acid, acetoacetic acid, and acetylacetone), NaCl and DDW into 15 mL polypropylene bottles. Prior to use, DDW was sparged with Ar overnight to eliminate inorganic carbonate. Sparging was continued during the duration of the experiments. The pH was set by the addition of HCl or NaOH. NaCl stock solution was added to ensure that the ionic strength was at least 1.0 mM. Given the other system constituents, the ionic strength is usually in the low mM range. A circulating

constant temperature bath maintained the temperature at 25.0 ± 0.2 ^{o}C. Stirring was performed using teflon-coated stir bars. Suspensions were equilibrated for two hours prior to filtration through 0.1 μm pore diameter track-etched polycarbonate filter membranes (Whatman). The concentrations of the test compound in the filtered solutions were analyzed using capillary electrophoresis (see later section).

A small number of adsorption experiments were conducted with the solid phase TiO_2. The extent of adsorption was obtained by subtracting the concentration measured in supernatant solution from the total added concentration. To confirm that degradation was not taking place, experiments were conducted where the testing compound was recovered from the TiO_2 surface by raising the pH to 12, which caused all three compounds to desorb.

4.3.3 Capillary Electrophoresis. A capillary electrophoresis unit from Beckman Coulter (P/ACE MDQ, Fullerton, CA) with diode-array UV-visible detector was used for all determinations. Bare fused silica capillaries (Polymicro Technologies, Phoenix, AZ) with 75 μm ID × 60 cm total length were used for all separations. The effective length, defined as the length from the inlet to the detector, was 52 cm. Between separations, the capillary was sequentially rinsed by flushing DDW for 0.5 minute, 0.1 N NaOH for 1 minute, DDW again for 1 minute, and capillary electrolyte for 2 minutes. Anion mode with constant applied voltage of -22 kV and -30 kV was employed for the direct and the indirect UV photometric methods, respectively.

A direct UV photometric method, with a CE electrolyte consisting of 20 mM pyrophosphate buffer (pH 7.5) and 0.4 mM tetradecyltrimethylammonium bromide (TTAB: Aldrich) electroosmotic flow modifier, was employed to analyze Mn^{III}(aq) (total

dissolved Mn^{III}) and described in detail elsewhere *(26)*. The pyrophosphate concentration is high enough and Mn^{III} sufficiently labile that all Mn^{III}-containing species in the sample are converted into Mn^{III}-pyrophosphate complexes upon contact with the CE electrolyte solution. A sharp, symmetrical peak, easily discernable at a detection wavelength of 235 nm, provided the means of measuring $Mn^{III}(aq)$ (total dissolved Mn^{III}). The detection limit for $Mn^{III}(aq)$ was about 1.5 μM at this wavelength.

CE electrolyte composition and detection wavelengths employed in the adsorption and oxidation experiments are provided in Table S4.2. Carbonyl groups are the only chromophoric groups for our analytes. Therefore, we have elected to use indirect photometric detection. Benzoate and phthalate both absorb light within a wavelength region convenient for CE (e.g. 200 to 230 nm). Displacement of these chromophoric anions by electromigrating analyte molecules yield negative peaks, which can be quantified. Tris or triethylamine are also added in the CE electrolyte to maintain constant pH.

4.3.4 Data Analysis. Initial rates of $Mn^{II}(aq)$ production (R_i, in units of μM/hr) were obtained from the slopes of concentration versus time plots. Unless otherwise stated, the slope corresponds to the least-squares fit of four or more data points collected during the first 15 % of dissolution. r^2 values were typically greater than 0.95.

When the pH was 5.0 or below, MnO_2 gradually released dissolved Mn^{II}, even in the absence of organic substrate. For results in the table below, only 200 μM MnO_2 and 10 mM buffer were present:

pH (buffer)	Dissolution Rate (μM/hr)	pH (buffer)	Dissolution Rate (μM/hr)
2.5 (self-buffering)	7.0×10^{-1}	4.0 (butyrate)	2.2×10^{-1}

3.0 (4-sulfobenzoate)	2.6×10^{-1}	4.5 (butyrate)	8.0×10^{-2}
3.5 (4-sulfobenzoate)	2.3×10^{-1}	5.0 (butyrate)	1.0×10^{-2}

When organic substrates are present, we will assume that the gradual release of $Mn^{II}(aq)$ just described proceeds in parallel. Dissolution rates arising from reaction with the organic substrate, which we will call R_0, are calculated by subtracting the background rates from R_i.

Protonation equilibria of organic substrates in homogeneous solution were calculated using the acidity constants listed in Tables 4.1 and 4.2, and the equilibrium program MINEQL+ *(29)*. Activity corrections to equilibrium constants were calculated using the Davis Equation (Stumm and Morgan *(30)*, page 103).

4.4 Results and Discussion

4.4.1 Adsorption Experiments. Substrate-to-substrate differences in extent of adsorption onto MnO_2(birnessite) will affect the overall redox reaction. Organic substrate adsorption onto MnO_2(birnessite) surface, however, cannot be studied due to the subsequent oxidation. Instead, the non-redox active TiO_2(rutile) is selected as the analogous surface for adsorption studies.

Figure 4.3 presents results for adsorption of 100 μM organic substrate (acetylacetone, acetoacetic acid, malonic acid, and dimethylmalonic acid) onto 5.0 g/L TiO_2(rutile) as a function of pH. Note that for all organic substrates, the maximum adsorption occurs near pK_a(s). Acetylacetone adsorption below pH 4.0 is less than measurable levels. The extent of adsorption gradually increases to a maximum as the pH is increased to 8.5, quite close to pK_a^{app} (9.00), and then gradually decreases as the pH is raised up to pH 12. Acetoacetic acid exhibits a plateau of maximum adsorption at pH

values below the pK_a (3.79). Increasing the pH above the pK_a causes adsorption to diminish. At pH 7.0, adsorption is below detectable levels. Malonic acid and dimethylmalonic acid adsorb in a similar manner. For both compounds, adsorption increases with increasing pH until a maximum is attained. Maximum adsorption pH region lies between pK_{a1} and pK_{a2}. Increasing pH above pK_{a2} causes adsorption to diminish to negligible levels at pH 8.

The maximum adsorption extents for acetylacetone, acetoacetic acid, malonic acid and dimethylmalonic acid are 27%, 25%, 87% and 66%, respectively. It is interesting to note that the maximum adsorptions for the β-dicarboxylic acids- malonic acid and dimethylmalonic acid are similar, but are much higher for the β-ketocarboxylic acid- acetoacetic acid and the β-diketone- acetylacetone.

What can be said about adsorption onto MnO_2(birnessite) based on what we have observed onto TiO_2(rutile)? TiO_2(rutile) is a non-ion exchanging phase with a pH_{zpc} of 6.1 *(31)*, structurally similar to AlOOH(boehmite) and FeOOH(lepidocrocite) *(32)*. MnO_2(birnessite) is a layered phase *(33)* with strong cation-exchange properties and a pH_{zpc} of 2.3 *(34, 35)*. In spite of the chemical differences of the two types of oxides, prior adsorption studies of carboxylate/phosphonate-based anions *(1, 36, 37)* and phosphate ion *(38)* indicate that the general trends of pH dependence for a specific anion adsorption onto the two types of (hydr)oxides are similar. In this study, we anticipate that substrate-to-substrate differences in the trend of pH dependence for adsorption onto MnO_2(birnessite) follows that observed with TiO_2(rutile).

4.4.2 Oxidation of b**-Dicarboxylic Acids.** *Malonic Acid, Methylmalonic Acid, and Dimethylmalonic Acid.* As shown in Table 4.2, R_0 values were obtained for

experiments employing 5.0 mM organic compound and 200 μM MnO_2 (pH 2.5 and 5.0). At both pHs, malonic acid and methylmalonic acid exhibit similar reactivities, with malonic acid slightly more reactive (within a factor of three). Malonic acid is, however, 120-times and 27-times more reactive than dimethylmalonic acid at pH 2.5 and 5.0, respectively. Dimethylmalonic acid exhibits the lowest pH dependence among the three.

As presented in an earlier section, malonic acid and dimethylmalonic acid adsorption onto TiO_2 exhibit similar pH dependence. The extents of adsorption with malonic acid are only 4-times and 1.3-times the values with dimethylmalonic acid at pH 2.5 and 5.0, respectively. If we assume that adsorption onto MnO_2 follows the trend with TiO_2, the small differences in adsorption cannot account for the significant reactivity differences. Hence, the reactivity differences most likely arise from the different electron transfer rates within the adsorbed species. Note that dimethylmalonic acid is the only compound among the three that does not possess an α-H. It is plausible to propose that, for malonic acid and methylmalonic acid, the presence of the α-H is responsible for the higher susceptibility to electron transfer within the adsorbed species.

Proposed Mechanism for Malonic Acid Oxidation. As shown in the proposed mechanism for malonic acid oxidation by MnO_2 (Figure 4.4), a total of six organic intermediates/products may form during reaction. Using capillary electrophoresis, analytical methods have been successfully developed for all organics listed in Figure 4.4, with detection limits 1-5 μM. Inorganic carbonate, which is believed to be an oxidation product for malonic acid, is not discernible by CE. For reaction samples, owing to the high resolution power of CE, any peak that grows upon addition of authentic standard is considered positively identified.

As illustrated in a time course plot (Figure 4.5a), reaction of malonic acid with MnO_2 only yields oxalic acid and formic acid in detectable quantities. Concentrations of the other proposed organic intermediates, tartronic acid, ketomalonic acid, glyoxylic acid, and glycolic acid, are below detectable levels throughout reaction. There are two possible reasons for the insignificant concentrations of these intermediates: (i), the proposed intermediates are formed during reaction, but are consumed too fast, i.e. too reactive to accumulate concentrations high enough for CE analysis; (ii), the proposed intermediates are not formed with the time scale of our experiments.

To test the two possible causes, R_0 values (initial $Mn^{II}(aq)$ production rates) are obtained from a separate set of experiments employing 5.0 mM of the organics listed in Figure 4.4 with 200 μM MnO_2 at pH 5.0. As shown in Figure 4.4, R_0 for tartronic acid, ketomalonic acid and glyoxylic acids are more than 340-times, for oxalic acid is 50-times, for glycolic acid is 1.6-times, and for formic acid is 0.2% that of malonic acid. The fact that glycolic acid is not detected but the more reactive oxalic acid is detected during malonic acid oxidation arises from (ii). More specifically, for the first two-electron oxidation of malonic acid, the decarboxylation pathway that yields glycolic acid is insignificant. An alternative pathway via conversion of α-hydrogen into α-hydroxyl group that yields tartronic acid is predominant. The fact that tartronic acid, ketomalonic acid and glyoxylic acid are not detected during malonic acid oxidation arises from (i), i.e. caused by their high reactivities. Reaction of tartronic acid with MnO_2 that yields appreciable glyoxylic acid, oxalic acid and formic acid (Figure 4.5b) further confirms our proposed mechanism for malonic acid oxidation. Once again, the undetectable ketomalonic acid is due to its extremely high reactivity. A similar reaction scheme has

also been proposed for malonic acid oxidation by Cr^{IV} *(39)* and by Mn^{III}-pyrophosphate *(40)* in homogeneous solutions, where tartronic acid has been identified as the sole two-electron-oxidation intermediate.

4.4.3 Oxidation of b**-Diketones.** The β-diketones listed in Table 4.1 were reacted at pH 2.5 and 5.0 with 200 μM MnO_2. A concentration of 5.0 mM β-diketone was employed. Initial rates with respect to Mn^{II}(aq) production (R_0) were obtained for comparison (Table 4.1). The reactivity rankings among all eight β-diketones are the same for reactions at both pHs: 3-chloro-2,4-pentandione > acetylacetone > 3,5-heptanedione > 3-ethyl-2,4-pentanedione > methyl acetoacetate > 1,1,1-trifluoro-2,4-pentanedione > 3,3-dimethyl-2,4-pentanedione > dimethyl malonate. At pH 5.0, the range of reactivity is approximately 2400-fold. At pH 2.5, the range of reactivity is far greater, more than 20,000-fold. As far as the effect of pH on R_0 is concerned, dimethyl malonate and 3,3-dimethyl-2,4-pentanedione, show very little pH dependence. For all the other compounds, R_0 values at pH 2.5 are in the range of 14 to 117 times higher than at pH 5.0.

The reactivity comparisons enable us to evaluate the relationships between reactivity and the keto-enol (and protonation) equilibria. Note that seven of the eight β-diketones possess α-H atom(s), including four γ-substituted β-diketones (3,5-heptanedione, methyl acetoacetate, 1,1,1-trifluoro-2,4-pentanedione, and dimethyl malonate), two α-substituted β-diketones (3-chloro-2,4-pentandione and 3-ethyl-2,4-pentanedione), and the non-substituted acetylacetone. For the γ-substituted β-diketones along with acetylacetone, R_0 values are higher for β-diketones with higher enol contents, although not in a linear fashion. The same trend also applies for the α-substituted β-

diketones along with acetylacetone. An α-substituted β-diketone exhibits a higher R_0 than a γ-substituted β-diketone with the similar enol content. For example, 3-ethyl-2,4-pentanedione and 1,1,1-trifluoro-2,4-pentanedione have similar enol content. 3-Ethyl-2,4-pentanedione is, however, 13-times and 8-times more reactive than 1,1,1-trifluoro-2,4-pentanedione. The K_E value for dimethyl malonate has not been reported because it is too low to measure. Dimethyl malonate is actually the least reactive β-diketone. The second least reactive β-diketone is 3,3-dimethyl-2,4-pentanedione, which does not have an α-H.

The higher MnO_2 reactivities for β-diketones with higher enol content indicates that the oxidation and enolization of β-diketones may share some traits in the fundamental processes. Since the correction between reactivity and enol content is not always good, we can conclude that substitution at α- and γ- positions affect them differently.

To explore the relationship between oxidation and enolization under the mechanistic level, we need to know more about the role of the α-CH in β-diketone degradation. Similarly to what we have observed with malonic acid oxidation, studies in aqueous solution *(41)* and organic solvents *(42-44)* show that the first two-electron oxidation leads to the conversion of an α-hydrogen into an α-hydroxyl group. The cleavage of the alpha C-H bond, via the donation of H atom, is proposed to be the key for oxidation *(14)*. The presence of a labile α-H for enolization is also crucial for H atom donating ability required for the oxidation. As with the rule of enol stabilization discussed in the Introduction section, a resonance effect allows delocalization of the unpaired electron and hence stabilizes α-C radicals created by H atom donation. The

stabilization of the α-C radicals decreases the activation energy for oxidation of β-diketones. Unlike enolization, where α-alkyl substituents decreases the enol content due to the steric hindrance, the greater number of α-alkyl substituents stabilizes α-C radicals *(45)*, and hence leads to higher susceptibility towards oxidation.

4.4.4 Acetylacetone, Acetoacetic Acid, and Malonic Acid. As shown in Figure 4.6, a detailed investigation was conducted on the effects of pH on the reaction of 200 μM MnO_2 with 5.0 mM organic substrate. Orders with respect to $[H^+]$ have been calculated as slopes between successive pairs of points on the $\log R_0$ versus pH plot (Figure 4.6). For all three substrates, R_0 decreases as the pH is increased. With acetoacetic acid and malonic acid, R_0 becomes more sensitive to $[H^+]$ as the pH is increased. For malonic acid, slopes increases from nearly 0.2 to 1.2 between pH 2.5 and 7.0. Acetoacetic acid yields steeper slopes than malonic acid up to pH 6.0. With acetylacetone, R_0 becomes less sensitive to $[H^+]$ as the pH is increased. From pH 2.5 to 7.0, slopes decrease from nearly 0.7 to 0.1. Consequently, the order of reactivity is pH dependent. Acetoacetic acid is the most reactive compound in the pH range of 2.5 to 4.5 and the least reactive compound at pH above 6. Acetylacetone and malonic acid have the same rates at pH 2.5. Upon raising the pH, acetylacetone exhibits lower rates than malonic acid until pH 6, but becomes more reactive than malonic acid near pH 7.

Combining the observed pH effect on reactivity in this section with the pH effect on adsorption in section 4.4.1 (Adsorption Experiments), reactivity that arises from the balance of adsorption and the subsequent electron transfer within the adsorbed species is clearly seen. A plausible explanation is that lower pH accelerates electron transfer of surface precursor species for all three organics. For acetylacetone, the unfavorable

adsorption at lower pH partially offsets the favorable electron transfer. For acetoacetic acid, both adsorption and electron transfer are more favorable at lower pH. For malonic acid, maximum adsorption occurs in the middle pH range. Adsorption starts to drop at pH below 3, resulting in the very gradual increase in rate with decreasing pH.

Oxidation of acetylacetone and malonic acid occurs at the α-C site has been proposed, where the liability of the α-H is the key. Since enolization is also dependent on the liability of the α-H, the order of electron transfer rate within the adsorbed species may be predicted based on K_E values, i.e. acetylacetone > acetoacetic acid > malonic acid.

4.4.5 Carboxylic Acids versus Their Esters. Malonic acid is more reactive than the corresponding esters, and the reactivity decreases in the order: malonic acid > methyl malonate > dimethyl malonate. Acetoacetic acid is more reactive than its ester, methyl acetoacetate. The binding of the carbonyl oxygen of esters is much weaker than the binding of a free carboxylic group towards metal ions *(46)*, which may cause less adsorption. However, the diminished reactivities for esters are also observed in aqueous solution *(46)*, indicating electronic effects that govern the susceptibility to electron transfer are responsible, rather than differences in adsorption properties.

4.5 Literature Cited

(1) Wang, Y. and Stone, A. T. Reaction of $Mn^{III,IV}$ (hydr)oxides with oxalic acid, glyoxylic acid, phosphonoformic acid, and structurally-related organic compounds. *Submitted to Geochim. Cosmochim. Acta*.

(2) Fox, T. R. and Comerford, N. B. Low-molecular-weight organic-acids in selected forest soils of the southeastern USA. *Soil Sci. Soc. Am. J.* **1990**, 54, 1139-1144.

(3) Madigan, M. T., Martinko, J. M., and Parker, J. *Brock Biology of Microorganisms*. 10th ed. 2002, Upper Saddle River, NJ: Prentice Hall.

(4) Afif, E., Barron, V., and Torrent, J. Organic-matter delays but does not prevent phosphate sorption by Cerrado soils from Brazil. *Soil Sci.* **1995**, 159, 207-211.

(5) Kirk, R. E. and Othmer, D. F. *Kirk-Othmer Encyclopedia of Chemical Technology*. 2004, New York: John Wiley.

(6) Sievers, R. E. and Sadlowski, J. E. Volatile metal-complexes. *Science* **1978**, 201, 217-223.

(7) Ozel, M. Z., Burford, M. D., Clifford, A. A., Bartle, K. D., Shadrin, A., Smart, N. G., and Tinker, N. D. Supercritical fluid extraction of cobalt with fluorinated and non-fluorinated β-diketones. *Anal. Chim. Acta* **1997**, 346, 73-80.

(8) Heimer, T. A., Darcangelis, S. T., Farzad, F., Stipkala, J. M., and Meyer, G. J. An acetylacetonate-based semiconductor-sensitizer linkage. *Inorg. Chem.* **1996**, 35, 5319-5324.

(9) Lewis, F. D., Miller, A. M., and Salvi, G. D. Spectroscopy and photochemistry of nickel(II), palladium(II), and platinum(II) β-diketonates. *Inorg. Chem.* **1995**, 34, 3173-3181.

(10) Venkateswarlu, S., Ramachandra, M., Rambabu, M., and Subbaraju, G. V. Synthesis of gingerenone-a and hirsutenone. *Indian J. Chem. B* **2001**, 40, 495-497.

(11) Nakano, K., Nakayachi, T., Yasumoto, E., Morshed, S., Hashimoto, K., Kikuchi, H., Nishikawa, H., Sugiyama, K., Amano, O., Kawase, M., and Sakagami, H. Induction of apoptosis by β-diketones in human tumor cells. *Anticancer Res.* **2004**, 24, 711-717.

(12) Adams, B. K., Ferstl, E. M., Davis, M. C., Herold, M., Kurtkaya, S., Camalier, R. F., Hollingshead, M. G., Kaur, G., Sausville, E. A., Rickles, F. R., Snyder, J. P., Liotta, D. C., and Shoji, M. Synthesis and biological evaluation of novel curcumin analogs as anti-cancer and anti-angiogenesis agents. *Bioorg. Med. Chem.* **2004**, 12, 3871-3883.

(13) Vajragupta, O., Boonchoong, P., Morris, G. M., and Olson, A. J. Active site binding modes of curcumin in HIV-1 protease and integrase. *Bioorg Med Chem Lett* **2005**, 15, 3364-3368.

(14) Jovanovic, S. V., Steenken, S., Boone, C. W., and Simic, M. G. H-atom transfer is a preferred antioxidant mechanism of curcumin. *J. Am. Chem. Soc.* **1999**, 121, 9677-9681.

(15) Jovanovic, S. V., Boone, C. W., Steenken, S., Trinoga, M., and Kaskey, R. B. How curcumin works preferentially with water soluble antioxidants. *J. Am. Chem. Soc.* **2001**, 123, 3064-3068.

(16) Toullec, J. Keto-enol equilibrium constant. In *The chemistry of enols*, Z. Rappoport, Editor. 1990, John Willey: Chichester, England. 323-398.

(17) Carey, F. A. and Sundberg, R. J. *Advanced Organic Chemistry*. 4th ed. 2000, New York: Plenum Press.

(18) Bunting, J. W., Kanter, J. P., Nelander, R., and Wu, Z. N. The acidity and tautomerism of β-diketones in aqueous-solution. *Can. J. Chem.***1995**, 73, 1305-1311.

(19) Iglesias, E. Application of organized microstructures to study keto-enol equilibrium of β-dicarbonyl compounds. *Curr. Org. Chem.* **2004**, 8, 1-24.

(20) Iglesias, E. Behavior of 1,1,1-trifluoroacetylacetone and 1,1,1-trifluoro-3-(2-thenoyl)acetone in aqueous micellar solutions of the cationic surfactants tetradecyltrimethylammonium bromide and tetradecyltrimethylammonium chloride. *Langmuir* **2000**, 16, 8438-8446.

(21) Alcais, P. and Brouillard, R. New data on keto-enol equilibria of 3-alkylpentane-2,4-diones in aqueous-solution. *J. Chem. Soc. Perk. T. 2* **1976**, 257-258.

(22) Perez, G. V. and Perez, A. L. Organic acids without a carboxylic acid functional group. *J. Chem. Educ.* **2000**, 77, 910-915.

(23) Kresge, A. J. Ingold lecture. Reactive intermediates: Carboxylic acid enols and other unstable species. *Chem. Soc. Rev.* **1996**, 25, 275-280.

(24) Field, R. J., Noyes, R. M., and Koros, E. Oscillations in chemical systems. 2. Thorough analysis of temporal oscillation in bromate-cerium-malonic acid system. *J. Am. Chem. Soc.* **1972**, 94, 8649-8664.

(25) Hansen, E. W. and Ruoff, P. Estimation of malonic-acid and methylmalonic acid enolization rate constants by an isotopic-exchange reaction using ^{1}H NMR spectroscopy. *J. Phys. Chem.* **1988**, 92, 2641-2645.

(26) Wang, Y. and Stone, A. T. The citric acid-$Mn^{III,IV}O2$(birnessite) reaction. Electron transfer, complex formation, and autocatalytic feedback. *Submitted to Geochim. Cosmochim. Acta* **2005**.

(27) Luo, J. A., Zhang, Q. H., and Suib, S. L. Mechanistic and kinetic studies of crystallization of birnessite. *Inorg. Chem.* **2000**, 39, 741-747.

(28) Giovanoli, R. and Leuenberger, U. Oxidation of manganese oxide hydroxide. *Helv. Chim. Acta* **1969**, 52, 2333-2347.

(29) Schecher, W. D. and McAvoy, D. C. *MINEQL+: A Chemical Equilibrium Modeling System*. 2003, Environmental Research Software: Hallowell, ME.

(30) Stumm, W. and Morgan, J. J. *Aquatic Chemistry -- Chemical Equilibria and Rates in Natural Waters*. 3rd ed. 1996, New York: John Wiley.

(31) Vasudevan, D. and Stone, A. T. Adsorption of 4-nitrocatechol, 4-nitro-2-aminophenol, and 4- nitro-1,2-phenylenediamine at the metal (hydr)oxide/water interface: Effect of metal (hydr)oxide properties. *J. Colloid Interf. Sci.* **1998**, 202, 1-19.

(32) Wells, A. F. *Structural Inorganic Chemistry*. 5th ed. 1984, Oxford, United Kingdom.: Clarendon Press.

(33) Post, J. E. and Veblen, D. R. Crystal-structure determinations of synthetic sodium, magnesium, and potassium birnessite using TEM and the Rietveld method. *Am. Mineral.* **1990**, 75, 477-489.

(34) Murray, J. W. Surface chemistry of hydrous manganese-dioxide. *J. Colloid Interf. Sci.* **1974**, 46, 357-371.

(35) Tonkin, J. W., Balistrieri, L. S., and Murray, J. W. Modeling sorption of divalent metal cations on hydrous manganese oxide using the diffuse double layer model. *Appl. Geochem.* **2004**, 19, 29-53.

(36) Kummert, R. and Stumm, W. The surface complexation of organic-acids on hydrous γ-Al_2O_3. *J. Colloid Interf. Sci.* **1980**, 75, 373-385.

(37) Nowack, B. and Stone, A. T. Adsorption of phosphonates onto the goethite-water interface. *J. Colloid Interf. Sci.* **1999**, 214, 20-30.

(38) Yao, W. S. and Millero, F. J. Adsorption of phosphate on manganese dioxide in seawater. *Environ. Sci. Technol.* **1996**, 30, 536-541.

(39) Senapati, M., Panigrahy, G. P., and Mahapatro, S. N. Pathways in chromic-acid oxidations. 3. Kinetics and mechanism of oxidation of malonic-acid. *J. Org. Chem.* **1985**, 50, 3651-3655.

(40) Drummond, A. Y. and Waters, W. A. Stages in oxidations of organic compounds by potassium permanganate. 4. Oxidation of malonic acid and its analogues. *J. Chem. Soc.* **1954**, 2456-2467.

(41) Gupta, M., Saha, S. K., and Banerjee, P. Kinetics and mechanism of the oxidation of ethyl acetoacetate and diethyl malonate by dodecatungstocobaltate(III). *B. Chem. Soc. JPN* **1990**, 63, 609-613.

(42) Adam, W. and Smerz, A. K. Nickel-catalyzed hydroxylation of 1,3-dicarbonyl compounds by dimethyldioxirane. *Tetrahedron* **1996**, 52, 5799-5804.

(43) Watanabe, T. and Ishikawa, T. Mild air-oxidation of 1,3-dicarbonyl compounds with cesium salts: Novel α-hydroxylation accompanied by partial hydrolysis of malonate derivatives. *Tetrahedron Lett.* **1999**, 40, 7795-7798.

(44) Toullec, P. Y., Bonaccorsi, C., Mezzetti, A., and Togni, A. Expanding the scope of asymmetric electrophilic atom-transfer reactions: Titanium- and ruthenium-catalyzed hydroxylation of β-ketoesters. *P. Natl. Acad. Sci. USA* **2004**, 101, 5810-5814.

(45) Perkins, M. J. *Radical Chemistry*. Ellis horwood series in organic chemistry. 1994, New York: Ellis Horwood.

(46) Deng, B. L. and Stone, A. T. Surface-catalyzed chromium(VI) reduction: The TiO_2-Cr^{VI}-mandelic acid system. *Environ. Sci. Technol.* **1996**, 30, 463-472.

(47) Koshimura, H., Okubo, T., and Saito, J. Effect of substituents on keto-enol equilibrium of alkyl-substituted β-diketones. *B. Chem. Soc. JPN* **1973**, 46, 632-634.

(48) Martell, A. E., Smith, R. M., and Motekaitis, R. J. *NIST Critically Selected Stability Constants of Metal Complexes Database*. 2004, US Department of Commerce, National Institute of Standards and Technology: Gaithersburg, MD.

(49) Bunting, J. W. and Kanter, J. P. Acidity and tautomerism of β-keto-esters and amides in aqueous-solution. *J. Am. Chem. Soc.* **1993**, 115, 11705-11715.

(50) *pK_a Value Calculated Using Advanced Chemistry Development (ACD) Software Solaris v4.67 (1994-2004) being cited by the electronic database SciFinder Scholar*.

(51) Chiang, Y., Guo, H. X., Kresge, A. J., and Tee, O. S. Flash photolysis of 2,2,6-trimethyl-4h-1,3-dioxin-4-one in aqueous solution: Hydration of acetylketene and ketonization of acetoacetic acid enol. *J. Am. Chem. Soc.* **1996**, 118, 3386-3391.

Table 4.1. Properties and MnO_2 Reactivity Comparisons Among b-Diketones

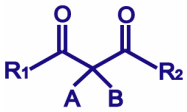

Chemical Name	Substituent				K_E	Ref.	pK_a^{app} (a-CH)	Ref.	R_0[1] (mM/h)		$R_{0,rel}$[2] (mM/h)
	R_1	R_2	A	B					pH 2.5	pH 5.0	
acetylacetone	CH_3	CH_3	H	H	$10^{-.069}$ $10^{-0.636}$	*(21)* *(47)*	9.00	*(48)*	60	3.4	17.6
3,5-heptanedione	C_2H_5	C_2H_5	H	H	$10^{-0.602}$	*(47)*	10.04	*(48)*	59	1.7	34.7
methyl acetoacetate	CH_3	OCH_3	H	H	$10^{-1.10}$	*(49)*	10.83	*(49)*	35	0.30	117
1,1,1-trifluoro-2,4-pentanedione	CH_3	CF_3	H	H	$10^{-1.91}$	*(20)*	6.33	*(48)*	3.0	0.14	21.4
dimethyl malonate	OCH_3	OCH_3	H	H			12.9	*(18)*	0.10	0.06	1.67
3-chloro-2,4-pentanedione[3]	CH_3	CH_3	Cl	H	$<10^{-.069}$		6.77	*(50)*	>2000	145	>13.8
3-ethyl-2,4-pentanedione	CH_3	CH_3	C_2H_5	H	$10^{-2.04}$	*(21)*	11.34	*(48)*	41	1.2	34.2
3,3-dimethyl-2,4-pentanedione	CH_3	CH_3	CH_3	CH_3					0.25	0.17	1.47

[1] The initial reaction rates (R_0) were obtained by reacting 5.0 mM substrate with 200 µM MnO_2(s) suspensions. pH maintained at 2.5 by self-buffering, at 5.0 by adding 10 mM butyrate. [2] $R_{0,rel}$ refers to relative rate at pH 2.5 versus at pH 5.0. [3] K_E value is estimated based upon the theory that the electron withdrawing chloro substituent in 3-chloro-2,4-pentanedione should increase the enol content comparing to acetylacetone *(16, 19)*.

Table 4.2. Properties and MnO_2 (or MnOOH) Reactivity Comparisons Among b-Ketocarboxylic Acids and b-Dicarboxylic Acids

Chemical Name	Structure	pK_as[1] (-COOH)	R_0[2] (mM/h)		$R_{0,\,rel}$[3] (mM/h)
			pH 2.5	pH 5.0	
acetoacetic acid	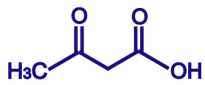	3.79	651	4.4	148
malonic acid, methyl ester	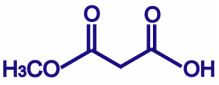	2.83 ± 0.20 [4]	11.3	0.51	22
malonic acid	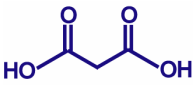	2.85 5.70	58	8.8	6.6
methylmalonic acid	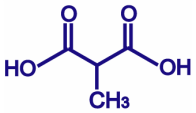	3.01 5.76	19.8	6.3	3.1
dimethylmalonic acid	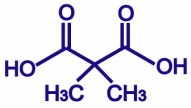	3.17 6.06	0.48	0.32	1.5

[1] All pK_a values from electronic database CRITICAL *(48)*, and referred to 25°C and zero ionic strength condition except otherwise mentioned. [2] The initial reaction rates (R_0) were obtained by reacting 5.0 mM substrate with 200 µM MnO_2 suspensions. pH maintained at 2.5 by self-buffering, at 5.0 by adding 10 mM butyrate. [3] $R_{0,\,rel}$ refers to relative rate at pH 2.5 versus pH 5.0. [4] pK_a value obtained from ACD software linked to the electronic database SciFinder *(50)*.

Keto-Enol Equilibria

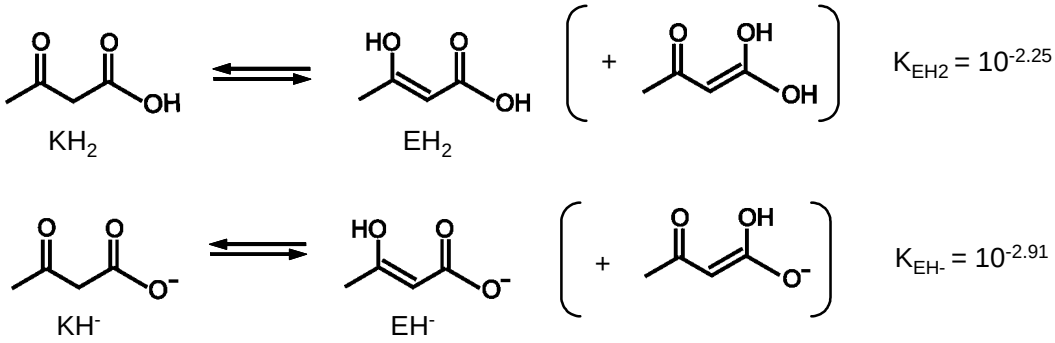

Acidity Constants

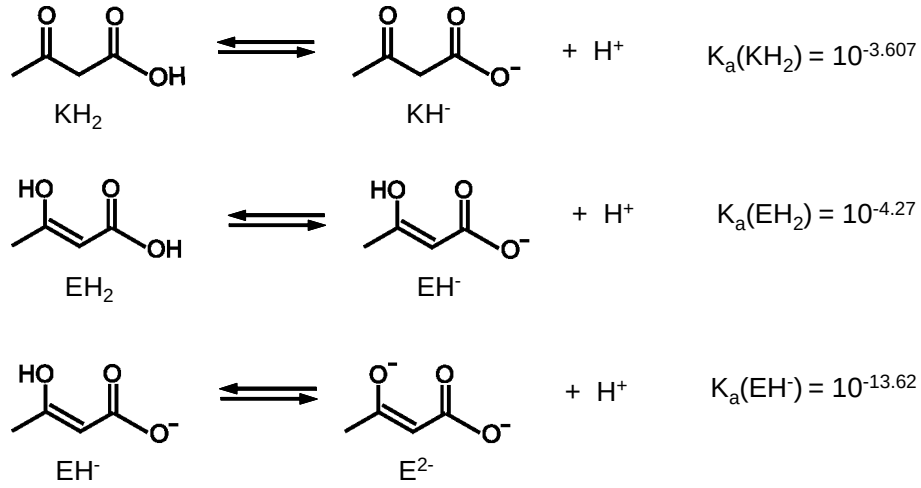

Figure 4.1. Acetoacetic acid equilibria at 25 ^{o}C and an ionic strength of 0.0 M, from Chiang et al. *(51)*. The enol isomers in the brackets are several orders of magnitude less abundant than the enol isomers on their left and can be ignored.

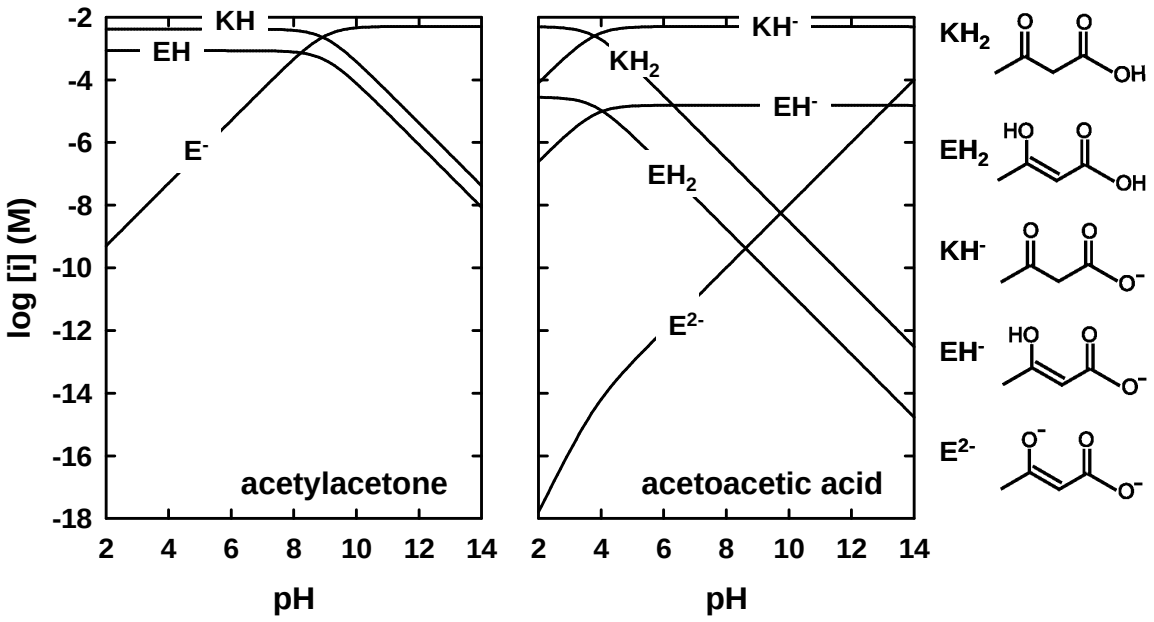

Figure 4.2. Equilibrium speciation of 5 mM acetylacetone and acetoacetic acid as a function of pH.

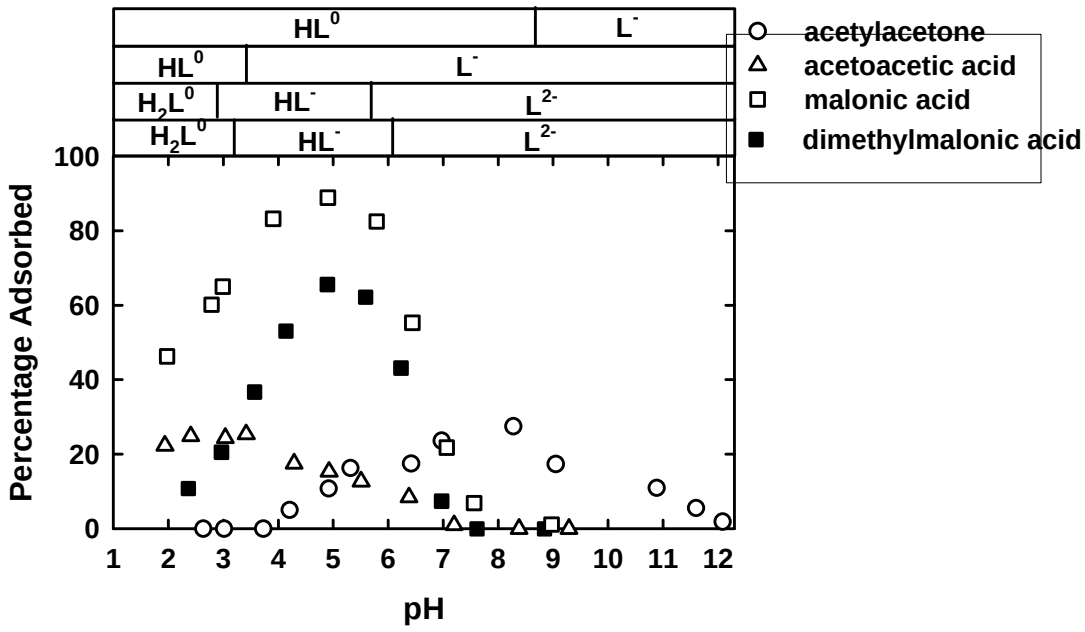

Figure 4.3. Adsorption of 100 mM organic substrates onto 5.0 g/L TiO_2 as a function of pH. All suspensions contained 1.0 mM NaCl. pH was set using HCl/NaOH addition. Top: Four bars denote predominant protonation level domains (at an ionic strength of 1.0 mM).

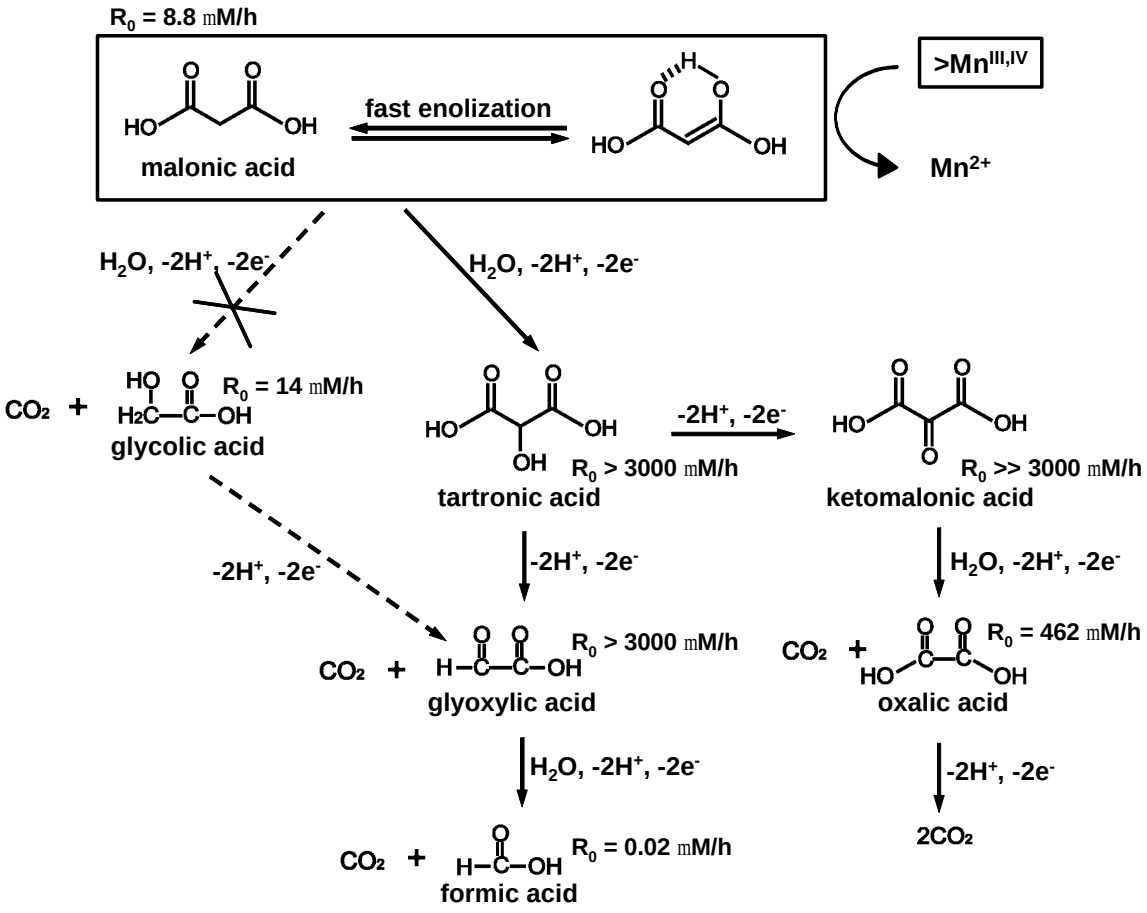

Figure 4.4. Proposed mechanism for malonic acid oxidation by MnO_2. R_0 refers to the initial rate with respect to Mn^{2+}(aq) production for reacting 5.0 mM organics with 200 mM MnO_2 at pH 5.0 (10 mM butyrate).

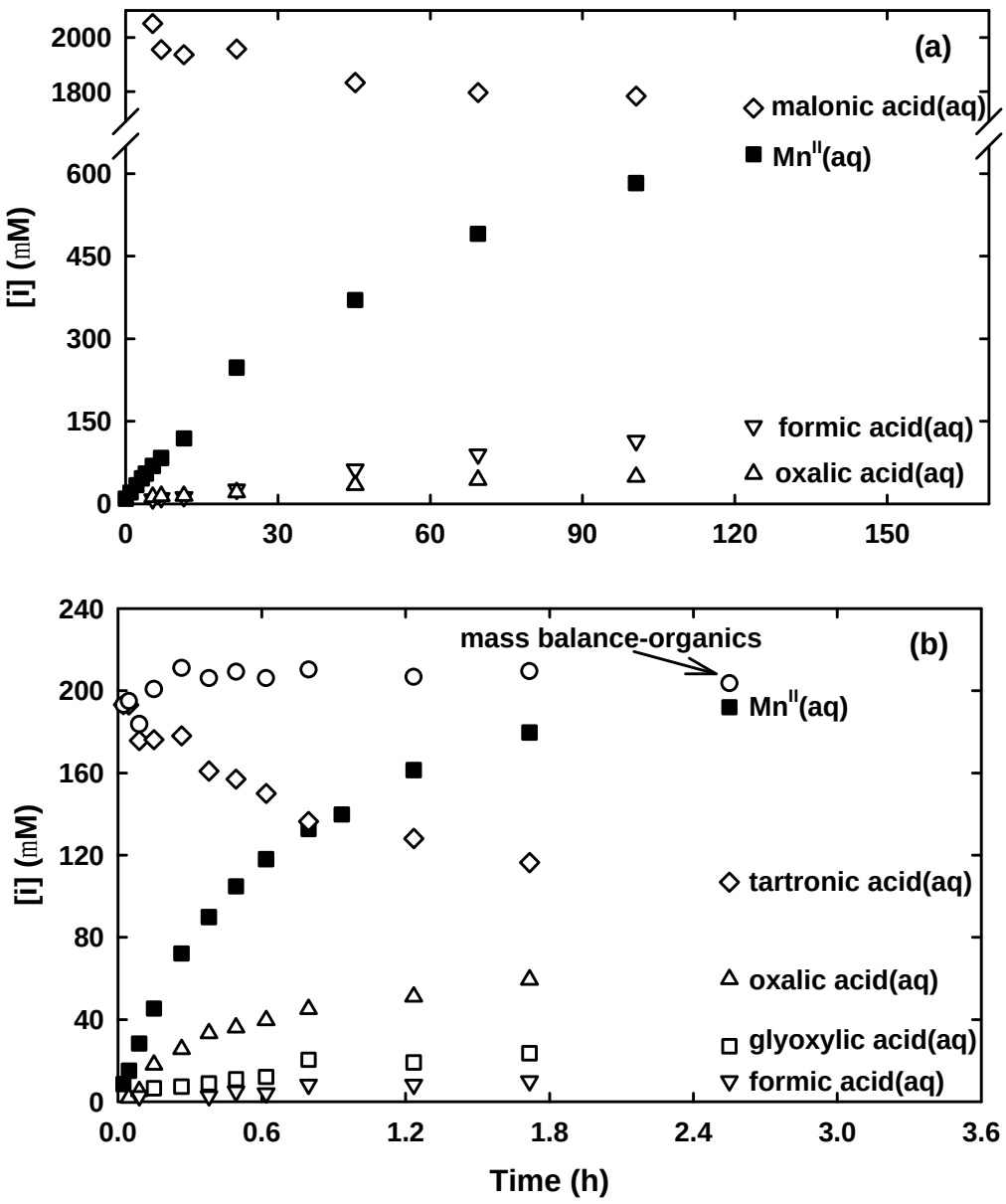

Figure 4.5. Reaction of (a) 2.0 mM malonic acid and (b) 200 mM tartronic acid with 200 mM MnO_2 at pH 5.0 (10 mM butyrate buffer). The mass balance in (b) refers to the sum [tartronic acid(aq)] + [oxalic acid(aq)] + [glyoxylic acid(aq)] + [formic acid(aq)].

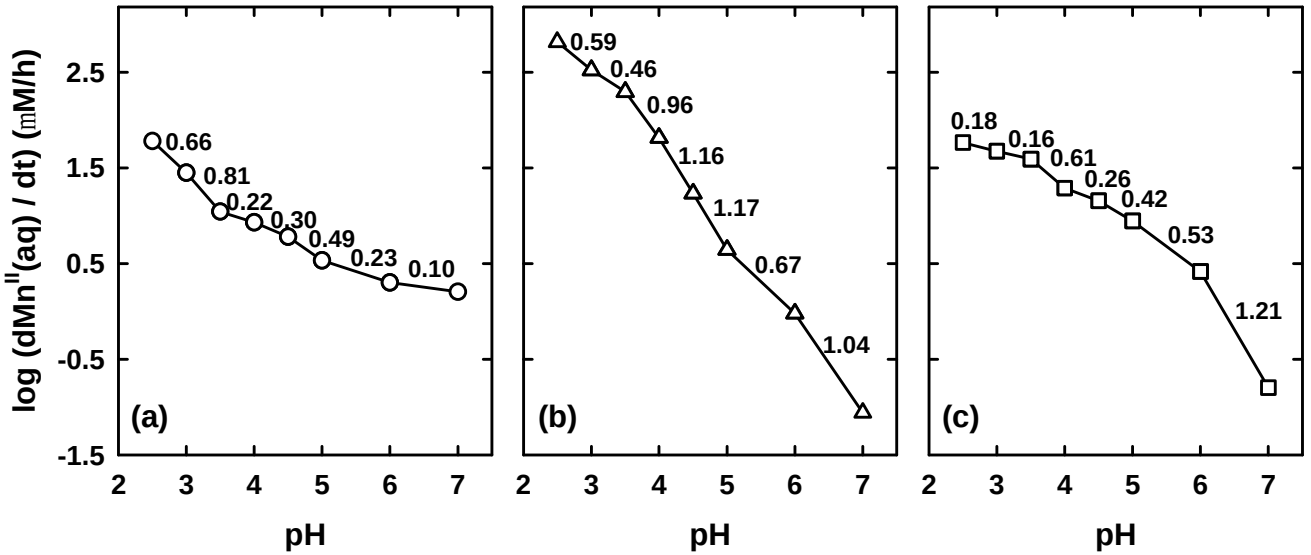

Figure 4.6. Effect of pH on (a) acetylacetone, (b) acetoacetic acid and (c) malonic acid oxidation by MnO_2. The order with respect to $[H^+]$ is calculated using successive pairs of points in the log-log plot. Reaction conditions: 5.0 mM organic, 0.2 mM MnO_2, and 10 mM pH buffer (4-sulfobenzoate for pH 3.0 and 3.5; butyrate for pH 4.0, 4.5, and 5.0; MES for pH 6.6; MOPS for pH 7.0).